JOURNAL OF MATERIALS SCIENCE 29 (1994) 4906–4912

Investigation into fracture mechanisms of, and the effect of stretch-straightening on an extruded metal-matrix composite

P. WILLIAMS, S. CANNON, B. RALPH
Department of Materials Technology Brunel University, Uxbridge, UB8 3PH, UK

A study has been made on samples of an extruded metal-matrix composite with an aluminium alloy (2124) matrix reinforced by 17.8% silicon carbide particles. Samples were straightened (plastically stretched) before performing tensile and compact tension tests. Fractographic analysis was affected using SEM analysis on single and matching faces. It was found that the ultimate tensile strength in the transverse direction decreased substantially (~45 MPa) on stretching and that the fracture toughness was influenced by the quenching rate. Further, the longitudinal and transverse ductilities were found to decrease and increase, respectively, with increasing plastic stretch. The SEM analysis supported a fracture mechanism where particles either fractured or decohered ahead of the crack tip with ductile failure of the matrix between the crack tip and the damaged particles.

1. Introduction

The development of metal-matrix composites (MMCs) has been spurred on by the need for structural materials with high specific stiffness and strength, particularly in the aerospace industry. The addition of a discontinuous reinforcement to a base-alloy matrix confers substantial improvements in specific modulus and strength over the values of the matrix material. However, the values of fracture toughness and ductility tend to be less than the unreinforced alloy. Consequently, an effort has been devoted to understanding the deformation and fracture mechanisms from a microstructural point of view in order to identify possible sources of weakness [1].

Particulate MMCs can be extruded in a very similar manner to an unreinforced alloy though little work has been done on the effect of extrusion on MMCs and how the mechanical properties of the material are affected by the subsequent straightening operations normally required after extrusion.

Thus, this study attempts to investigate:

1. the fracture mechanism that operates in a particular MMC by examination of matching fracture faces; and
2. the effect of stretch straightening on the mechanical properties of extruded product by simulating the stretching on sections of such an extrusion.

1.1. Investigation of the crack path

Taking an aluminium alloy with silicon carbide reinforcement as an example, the interfacial bonding between the matrix and the particles is considered to be very good [2, 3], thus allowing good load transfer to occur between the aluminium and the silicon carbide. However, the microstructural evidence for precise fracture initiation and propagation is not clear. The crack path needs to be identified; whether it is between the particles in the matrix only (Fig. 1a), through the particles (Fig. 1b), or, in spite of the good bonding, at the interface (Fig. 1c).

From the examination of matching fractographs it may be possible to identify the crack path and fracture mechanism. This effect has been noted previously by Roebuck in a similar experiment, and he stresses the importance of not drawing conclusions on fracture mechanisms from a single fracture face [4].

1.2. Stretch straightening of extrudate

As it emerges from the die, most metallic extruded product is bent or curved in nature along its longitudinal axis. This is normally remedied by subsequent secondary processing to stretch straighten the extrudate. This process involves applying a plastic stretch to the longitudinal axis. As the intrinsic ductility of the MMC material is low, some concern has been expressed as to the effect of such stretch straightening on the composite material.

This report attempts to simulate this process on such a composite material and to analyse its effect on the tensile and fracture toughness properties.

2. Experimental procedure

2.1. Material and production process

The material under investigation was a silicon carbide-reinforced aluminium-matrix composite, sup-

0022–2461

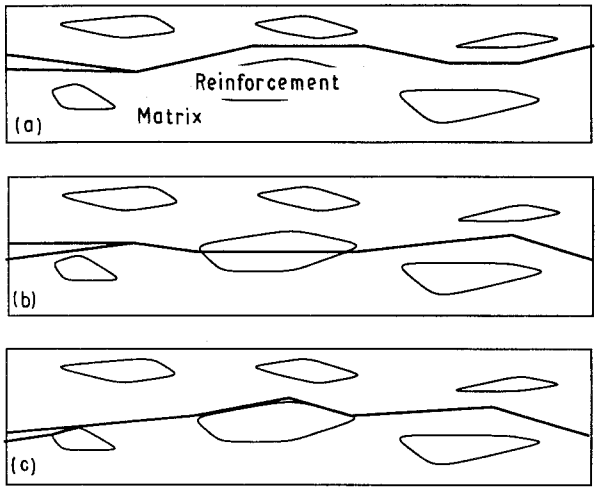

Figure 1 A schematic illustration of possible fracture paths through a particulate-reinforced metal-matrix composite. (a) Crack proceeds through matrix only. (b) Crack path proceeds through matrix and reinforcement. (c) Crack path proceeds through matrix and at the interface.

plied by BP Metal Composites (now Aerospace Metal Composites). The proportion of SiC reinforcement to aluminium matrix was 17.8% by volume. The matrix alloy was a 2124 aluminium powder. The particulate reinforcement was a fine 3 μm sized black silicon carbide powder, grade C6 F1200. The billet was prepared using a powder metallurgy process to produce a non-fully dense billet, followed by hot isostatic pressing (HIP) to densify the billet fully.

The 23 kg billet was extruded at IMI Titanium Ltd, Birmingham, to a bar 5.9 m long with a cross-section of 75 mm × 18 mm. All sides had a good surface finish with slight longitudinal scoring on all faces.

Three 30 cm lengths, taken from the centre of this bar, underwent a heat treatment at 505 °C and then quenching in a cold-water bath. Two of the 30 cm sections were stretched within 2 min of being removed from the oven. One section was retained as a control.

The stretching was performed immediately after quenching, to prevent the material age hardening before the stretching commenced. On the first bar, a stress of 360 MN m^{-2} was applied and the final plastic stretch was 0.5%. On the second bar the entire capacity of the machine was employed (500 kN) to give a stress of 370 MN m^{-2}, which resulted in a 1% plastic stretch.

2.2. Tensile tests, compact tension tests, and microstructural evaluation

Polished sections of the un-heat-treated bar were viewed under an optical microscope to analyse the particle distribution. Tensile tests were performed on the as-extruded material in the longitudinal and transverse orientations.

Two types of mechanical tests were performed on the heat-treated material, tensile and compact tension. Tensile specimens were machined from the three lengths in longitudinal and transverse orientations. The tests were performed in accordance to the British Standard BS 18 [5]. Values for ultimate tensile strength, 0.2% yield strength and ductility were measured.

Compact tension samples were also machined in the longitudinal and transverse orientations with dimensions in proportion to a net width of 19 mm, as stated in BS5447 [6]. BS 5447 requires that an atomically sharp crack be produced at the tip of the notch to act as a precrack to ensure the main crack propagates in a direction perpendicular to the load axis. This is normally achieved by fatigue methods although it has been shown that certain machined cracks can achieve the same result [7]. Similar to work done by Mummery and Derby [8], in this study the notch was introduced by spark erosion to prevent mechanical damage to the root notch.

Both the compact tension and tensile specimen fracture surfaces were examined using a scanning electron microscope (SEM). The tensile specimens were examined on one face only. With the compact tension samples, matching fracture surfaces were examined and corresponding areas on both sides of the fracture were located and photographed.

3. Results

Examination of polished as-extruded material by light microscopy revealed that the material had a homogeneous distribution of SiC particles within the matrix. A composite micrograph showing all three orientations of the material is given in Fig. 2.

The single fracture face micrographs (Fig. 3a and b) show a silicon carbide concentration on the fracture surface slightly lower than that noted on a random polished surface. Almost all of the SiC particles visible on the fracture surfaces are cracked (Fig. 3a–d). These micrographs reveal fractured SiC particles at the base of dimples surrounded by ductile fracture of the matrix. The matrix and the reinforcement can be distinguished by contrasting the dimpled topography of the matrix which fractured in a ductile manner, to the flat facet-like smooth surfaces of the brittle fractured reinforcement.

The matching fractographs also show a very high proportion of cracked SiC particles. In most cases, for each SiC particle found on one side of the fracture face, a corresponding fractured particle could be found on the other (Fig. 4a and b). Voids in the matrix were noted much less frequently.

A fractured silicon carbide particle, examined at high magnification (Fig. 4c) shows an obvious crack running across the centre of the particle. At the bottom of the particle are the beginnings of decohesion from the matrix at the interface.

The tensile test results from the as-extruded and stretched bars are given in Table I. Comparison of the tensile results from the control and stretched bars to the tensile results from the as-extruded product shows a marked decrease in the tensile strength, proof strength and ductility in the stretched and control

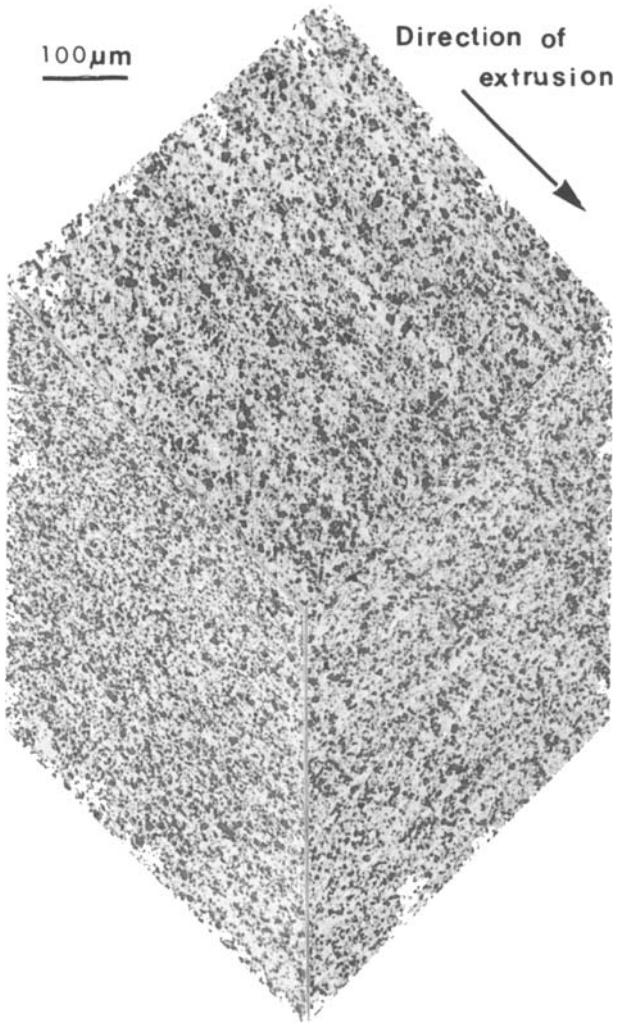

Figure 2 A composite light micrograph of three perpendicular faces of the as-extruded bar which reveals a relatively homogeneous microstructure.

material. As the control material, which has undergone no elastic or plastic deformation, also exhibits this decrease, the stretching must be ruled out as the cause and the heat treatment must be looked at as the affecting factor.

The load and extension at failure for the compact tension samples are given in Table II. Of the 12 samples tested, 11 broke on a fracture plane perpendicular to the load axis to within 5° as required in the standard. The twelfth sample, a 0.5% L sample, fractured at an angle of approximately 15°. All of the samples showed the shear lip/plateau fracture topography described by Knott [9] (Fig. 4d).

The compact tension samples showed almost perfectly elastic behaviour until fracture. The type of fracture in each case is almost entirely brittle and very little plastic deformation was noted in any of the samples. One of the control samples, L, showed an extension of almost twice that of all the other samples, caused by the bending of the steel pins during testing. The bent pins were noted following the test and all subsequent tests used 4.5 mm pins which showed no such tendency to bend. All the curves are Type III curves as defined by the British Standard [6] which

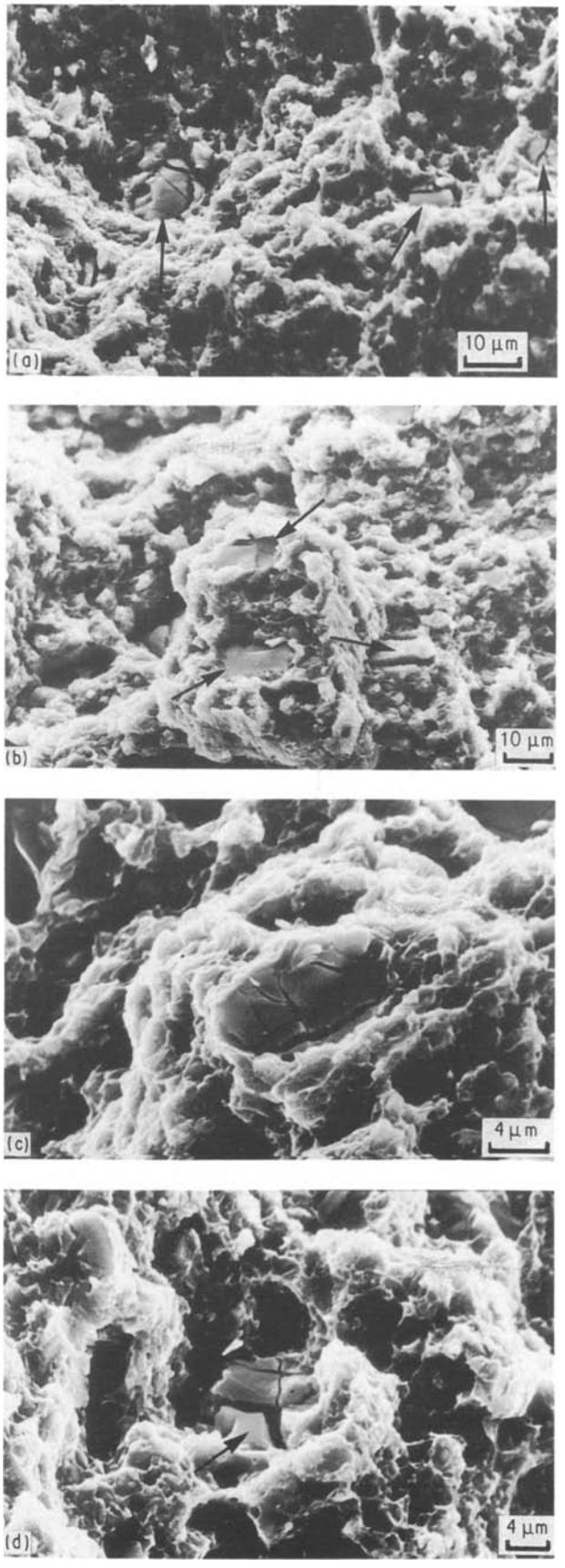

Figure 3 Scanning electron micrographs of single fracture faces: (a) from a tensile sample pulled to failure in the direction of extrusion (fractured silicon carbide particles are revealed and arrowed); (b) from a tensile sample pulled to failure in a direction transverse to the direction of extrusion (again fractured carbide particles are revealed and indicated); (c) as (b) but at higher magnification where a fractured silicon carbide particle is more obvious; (d) from a tensile sample pulled to failure in the direction of extrusion (in this case less matrix ductility is apparent; again a fractured silicon carbide particle is indicated).

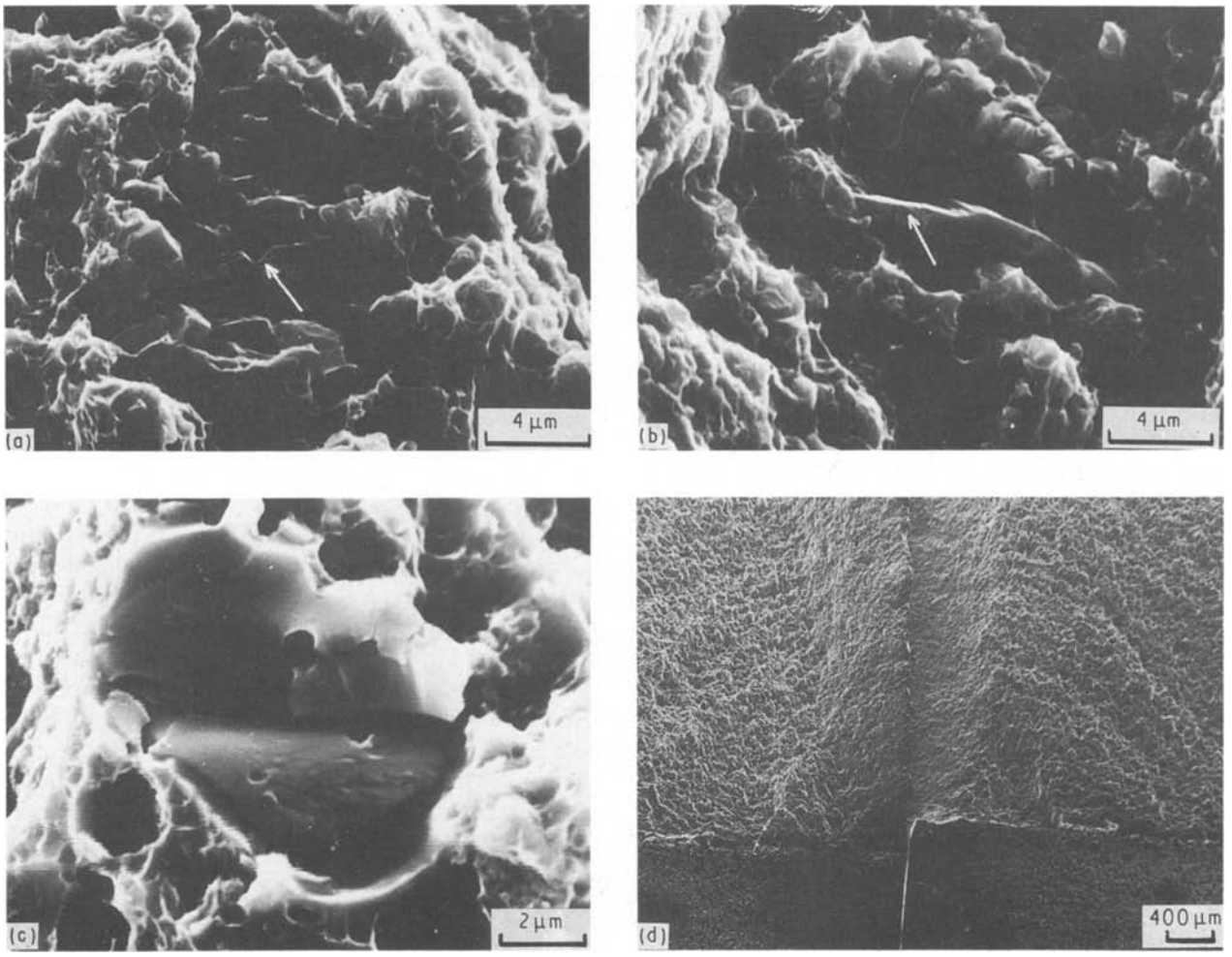

Figure 4 Scanning electron micrographs of fracture surfaces from compact tension samples. (a, b) Matching micrographs from both sides of the fracture surface. Here broken silicon carbide particles are seen on both faces and indicated. (c) Higher magnification of fractured silicon carbide particle suggesting some local decohesion from the matrix. (d) Composite showing two halves of a fractured specimen placed adjacent to each other and indicating the formation of shear lips.

TABLE I Tensile values for as extruded and stretched material

Bar	Orientation	Ultimate tensile strength (MPa)	0.2% proof strength (MPa)	Elongation (%)
As-extruded	L	637	430	7.7
As-extruded	T	593	427	5.2
Control	L	600	417	5
Control	T	564	406	4
0.5%	L	610	454	5
0.5%	T	536	462	4.5
1%	L	604	458	4.5
1%	T	520	418	4.5

TABLE II Compact tension test results for stretched material (including K_Q values and the calculated constraints)

Sample	Load at failure (kN)	Extension at failure (mm)	K_Q (MPa $m^{1/2}$)	$5(K_Q/\sigma_{ys})^2$ (m)
Control L	7.1	0.083	45.89	0.061
Control L	6.8	0.032	43.95	0.056
Control T	5.5	0.023	35.29	0.038
Control T	5.0	0.020	31.91	0.031
0.5% L	6.4	0.039	41.05	0.041
0.5% L	5.8	0.027	37.12	0.034
0.5% T	5.9	0.027	38.14	0.034
0.5% T	5.1	0.023	32.88	0.025
1% L	7.1	0.033	45.39	0.049
1% L	6.8	0.030	43.36	0.045
1% T	6.3	0.028	40.63	0.047
1% T	5.6	0.026	36.07	0.030

means that the P_Q value used in the calculation of K_Q is taken to be P_{max}, i.e. the load at failure.

Using the equations given in BS5447, K_Q can be found.

$$K_Q = 6420\, P_Q \text{ MPa m}^{1/2} \quad (1)$$

where $P_Q = P_{max}$, the K_Q values for the compact tension samples can be calculated. Table II gives the calculated K_Q values. The values required in the constraints for determining validity are also calculated, using the equations given. The value of σ_{ys} used is the 0.2% proof strength found in the tensile tests. These values are also given in Table II.

4.1. The effects of stretch straightening

Firstly, the discrepancy in mechanical properties between the as-extruded and stretched material must be considered. Comparison of the tensile results of the as-extruded and stretched material shows that the subsequent treatment of the extruded product leads to a sizeable decrease in all of the values of the mechanical properties obtained by the tensile tests. The stretching of the material can be ruled out as a cause of the decrease as the control was also affected. This leaves the heat treatment as the only other possible cause. Both the as-extruded bar and the control bar were given the same heat treatment regime prior to machining of the test pieces. The as-extruded product was quenched in water at room temperature and left to cool in the water. The control bar, and the material to be stretched, were quenched in a similar volume of water, but, the material was not allowed to cool in the water. Instead, it was removed and stretched (simply removed in the control case) whilst still hot to the touch. It would appear that it is this factor which led to a non-optimal heat treatment which caused the diminished properties.

By examining the results given in Table II, certain comments can be made about the effects of stretch straightening on the mechanical properties of this material. For instance, increasing the plastic deformation to 1% seems to have little effect on the transverse K_Q values and no trend emerges from the longitudinal values. The values for ultimate tensile strength in the longitudinal orientation are not greatly affected by the changes in plastic deformation to the material. However, a plastic stretch of 1% causes a 45 MPa decrease in the transverse ultimate tensile strength. As this value is already low, the decrease may be cause for alarm.

4.2. Discussion of K_Q and K_{IC} values, and fracture toughness

When a notched specimen is stressed below its yield stress, i.e. still in the elastic region, the notch acts as a stress concentrator that produces high stresses near the notch which may locally exceed the yield stress to produce a small plastic zone. The stress distribution in this zone depends on whether the deformation is occurring in plane stress or in plane strain. The plane stress situation occurs near the edges of the specimen where the constraints on the material are reduced in the through thickness or σ_{33} direction. Yielding occurs at 45° to the load axis by a shear mechanism [9, 10]. The plane strain situation occurs at the centre of the specimen where the constraints are approximately equal in all directions. The material cannot deform by a ductile mechanism and the specimen tears in a plane normal to the load axis.

The shear lips on the edges of the specimens (Fig. 4d) are formed by fracture in plane stress conditions whilst the plateau is formed by plane strain conditions. The fracture toughness of the material varies with the thickness of the sample in a manner depicted in Fig. 5. A minimum value of fracture

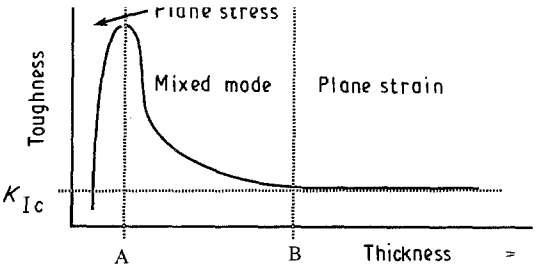

Figure 5 Schematic illustration of the variation of toughness with thickness of a specimen. In the geometry required in these experiments, the fracture was mixed mode and thus only K_Q values obtained.

toughness is achieved when the thickness increases to a certain value, B. This value for fracture toughness is termed K_{IC}, the critical stress intensity value of that material. Samples of thickness less than A are small enough that the edge effects remove the constraints in the σ_{33} direction throughout the entire thickness and the whole sample fails under plane stress conditions with a 45° fracture face. Samples of thickness greater than B are large enough for the effect of the reduced constraints at the edges to be minimal and the sample fails in a plane strain manner. It is for these samples that the K_{IC} values are valid.

Samples of thickness greater than A but less than B fail by mixed mode mechanism. The proportion of plane stress failure is enough to affect the toughness of the material to some extent. The shear lips require sufficient energy on formation to raise the fracture toughness of the material. The fracture toughness for that particular sample is referred to as K_Q. K_Q is the critical stress intensity factor for a particular thickness of a specified material and is always greater than or equal to K_{IC}. For example, Downes and King [11], using similar material with a 3 μm sized reinforcement, obtained average plane strain fracture toughness, K_{IC}, of 14.0 MPa $m^{1/2}$. This is considerably lower than the K_Q range of 30–45 MPa $m^{1/2}$ obtained in this investigation. The Downes and King results fall in the flat plane strain region of the curve in Fig. 5, whereas the K_Q values, by definition, fall into the mixed mode region and lie higher on the curve.

The size of specimens used in this investigation fell into the mixed mode category. The values are not valid K_{IC} values for the samples as the dimensions do not satisfy the constraints given in BS 5447 (see Table II).

Why were the samples the size they were and not bigger? The thickness of the extrusion was the major limiting factor, being only 18 mm. To avoid any zone effects there might be in the extruded bar, the samples were machined from the extrudate 4 mm from each edge. The eventual specimen thickness was 9.5 mm and the other dimensions were adjusted to reflect this and bring the samples in line with the specifications set out in BS 5447. As a result, the fracture toughness values determined in this study can only be reported as K_Q values. They are the fracture toughness for

would have lower values for fracture toughness. These results can be used to estimate the size of sample needed to obtain valid K_{IC} values in future work. BS5447 suggests that the width should be approximately equal to the largest value of the $5(K_Q/\sigma_{ys})^2$ constraint. The figures in Table II therefore suggest that the samples should be approximately 60 mm wide, with the other dimensions scaled accordingly.

4.3. Suggested fracture mechanisms

Published work [12–14], investigating only one side of the fracture surface, proposes that the fracture path preferentially avoids the reinforcement particles and that the fracture process was initiated by voids formed in the matrix close to the matrix/particle interface. These voids then linked by microvoid coalescence in the matrix between the SiC particles thus leading to overall fracture. However, few if any SiC particles would be visible on the fracture surface if the mechanism proceeded as described above. By contrast, silicon carbide particles are clearly visible in all of the fractographs taken above × 2000 magnification. The mechanism above cannot be used to describe adequately what is occurring in the materials tested in this study.

SiC particles were found on one side of the fracture for which no corresponding particle on the opposite face could be found. These particles could be regarded as having decohered from the matrix. This was noted less frequently than particle fracture. Some of the high magnification fractographs of the fractured particles show the beginnings of decohesion at the interface (Fig. 4c). This would imply that the interfacial bond strength and the strength of the particles were of similar magnitude, the particle strength being slightly lower, thus breaking preferentially. Individual local aspects, such as interfacial defects, would affect which mechanism prevailed for each particle.

The matching fractographs, single-face SEM analysis and the light microscopy analysis show that the SiC particles are splitting and decohering from the matrix, with only slightly less SiC on the fracture face than in the bulk material. It is proposed, therefore, that the crack path does not preferentially seek nor avoid the reinforcement, rather, takes a random path across the material, splitting or decohering any reinforcement encountered.

Two possible fracture mechanisms could result in the fracture faces observed.

(i) As proposed by You *et al.* [15], the dominant fracture mechanism is failure in the matrix. The reinforcement particles contribute to the failure process by imposing high levels of constraint on the matrix deformation. Cracking of the reinforcement occurs, but only as a result of matrix failure and the reinforcement supports all the load at failure.

(ii) A two-step mechanism similar to that suggested by Da Silva *et al.* [1] occurs, where the SiC particles break ahead of the crack tip followed by the linking of matrix.

4.4. Discussion of You *et al.*'s fracture mechanism

As a simple model of the extreme case of the proposed mechanism, You *et al.* [15] calculated the stress applied to the SiC particles in a tensile specimen, assuming complete matrix separation before fracture in a plane perpendicular to the load axis. This would result in the reinforcement bearing all the load. The stress was calculated by dividing the failure load by the area of the SiC particles on the fracture surface. That study obtained a value of 2.7 GPa. Repeating that calculation in the present work, taking the volume fraction of reinforcement to be the proportion of SiC on the fracture surface, gives

maximum load during tensile tests = 11 000 N

area of tensile specimen = $(2.5 \times 10^{-3})^2 \times \pi$

area of SiC on fracture face = area of tensile specimen × 17.8%

ultimate tensile stress of SiC = maximum load/area of SiC

$$= \frac{11\,000}{(2.5 \times 10^{-3})^2 \times \pi \times 17.8\%}$$

$$= 3.147 \times 10^9 \text{ Pa}$$

$$= 3.147 \text{ GPa}$$

Whilst the SiC/Al interface bond strength is considered to be very good, figures calculated by Flom and Arsenault [3] suggest that it is about 1.7 GPa, approximately half that of the figure calculated for the particle strength.

It could be expected from comparison of these figures that, on fracture, the reinforcement would decohere from the matrix in preference to breakage of the particles. From examination of the matching fracture surfaces, it is evident that this is not the case and that, in fact, the reverse occurs at least as often.

This suggests that either You *et al.*'s model for predicting the strength of the particles is too simplistic and that an important factor has been excluded, or the entire mechanism as suggested by You *et al.* needs adapting.

4.5. Discussion of Da Silva *et al.*'s mechanism

The alternative mechanism is that the crack induces very localized damage ahead of its tip. This damage includes splitting of the reinforcement and decohesion from the matrix. The crack advances by ductile fracture of the matrix as this localized damage causes excessive load to be placed on the matrix in front of the crack tip.

As the material is strained, the high strength of the matrix and the good load transfer through the interface ensure that the stresses on the reinforcement ahead of the crack tip are large. Fracture can then occur in the reinforcement via pre-existing flaws in the

particles, probably caused during fabrication of the billet or during extrusion. This is enhanced by the extremely brittle nature and the high notch sensitivity of the reinforcing phase, coupled with the high localized stress concentrations normally experienced just ahead of the crack tip. Once the reinforcement fractures, the net load-carrying capacity of the composite decreases. The ligament of matrix material between the crack tip and the now ruptured SiC particle fails by ductile fracture creating the characteristic dimpled effect, and the crack tip moves forward. This explanation matches that given by Mummery and Derby in an *in situ* study of failure of similar samples [8].

Owing to the large difference in stiffness between the aluminium and silicon carbide, stress concentrations arise in the matrix close to the Al/SiC interface. The presence of the fine particulate SiC in the matrix acts as a barrier to relief of this stress concentration by plastic deformation. Thus a number of microcracks are formed in the matrix near the particles when the macroscopic strain level is relatively low. Any interfacial defects, such as the presence of an AlC_4 phase on the interface for instance, could lead to interfacial decohesion of that particle.

5. Conclusion

The equipment and processes used in the pursuit of this study were insufficient to simulate accurately the stretch straightening of extruded silicon carbide-reinforced aluminium alloy. However, a plastic deformation of 0.5% and 1% was imparted to extruded sections. These sections were then subjected to tensile tests, compact tension tests, and matching fracture face SEM analysis. Various observations were made from these tests and this analysis.

The rapid removal of the heat-treated bars from the quench tank, necessitated by the need to stretch before the onset of excessive age hardening, leads to a negative effect on the tensile properties.

The cooling rate experienced during quenching has a pronounced effect on the fracture toughness of the material. Displacement from the edge of quenched material will have an effect on the toughness, highest toughness occurring closest to the edge.

Values of ultimate tensile strength in the longitudinal direction were not greatly effected by the small amount of plastic deformation imparted to the material. However, the ultimate tensile strength in the transverse direction saw a substantial decrease, a factor which may be cause for some concern.

The ductility decreased in the longitudinal direction and increased in the transverse direction with increasing stretch, broadly as expected.

Valid K_{IC} values could not be quoted for fracture toughness due to the nature of the notch and size of the test pieces. Instead K_Q values were determined. Valid K_{IC} values cannot be obtained for the extruded bar as the critical width factor needed is greater than the width of the bar.

A mechanism for fracture in the material has been proposed. The SiC reinforcement fractures or decoheres from the matrix material in a region ahead of the advancing crack tip. The crack tip advances by ductile fracture of the ligament of matrix material between the crack tip and the now fractured or decohered reinforcement particle.

Acknowledgements

The authors thank BP Metal Composites (now Aerospace Metal Composites) for the supply of material, and the Experimental Techniques Centre, Brunel University, for technical assistance.

References

1. R. DA SILVA, D. CALDEMAISON and T. BRETHEAU, in "9th RISØ International Symposium on Metallurgy and Materials Science"edited by S. I. Anderson, H. Lilholt and O. B. Pedersen : (RISØ, Roskilde, Denmark, 1988) pp. 333–8.
2. S. DOONG, T. LEE, I. ROBERTSON and H. BIRNBAUM, *Scripta Metall.* **23** (1989) 1413.
3. Y. FLOM and R. ARSENAULT, *Mater. Sci. Engng* **77** (1986) 191.
4. B. ROEBUCK, *J. Mater. Sci. Lett.* **6** (1987) 1138.
5. BS 18, 1987 British Standards Institution, "Methods for tensile testing of metals" (1987) (withdrawn), replaced by BS EN 10002: 1990 British Standards Institution, "Tensile testing of metallic materials" (1990).
6. BS 5447: 1977 British Standards Institution, "Plane strain fracture toughness of metallic materials" (1977).
7. M. MANOHARAN, and J. LEWANDOWSKI, *Acta. Metall. Mater.* **38** (1990) 489.
8. P. MUMMERY and B. DERBY, in "12th RISØ International Symposium on Materials Science" edited by N. Hansen, D. Juul Jensen, T. Leffers, H. Lilholt, T. Lorentzen, A. S. Pedersen, O. B. Pedersen and B. Ralph. (RISØ, Roskilde, 1991) pp. 535–542.
9. J. KNOTT, "Fundamentals of fracture mechanics" (Butterworths, London, 1973).
10. S. ROLFE, and J. BARSOM, "Fracture and fatigue Control in Structures" (Prentice-Hall, New York, 1977).
11. T. DOWNES, and J. KING, in "12th RISØ International Symposium on Materials Science" edited by N. Hansen, D. Juul Jensen, T. Leffers, H. Lilholt, T. Lorentzen, A. S. Pedersen, O. B. Pedersen and B. Ralph. (RISØ, Roskilde, 1991) pp. 305–10
12. R. ARSENAULT and C. PANDE, *Scripta Metall* **18** (1984) 1131.
13. Y. FLOM and R. ARSENAULT, *J. Metals* July **38** (1986) 31.
14. C. CROWE, R. GRAY and D. HASSON, 5th International Conference on Composite Materials (AIME, 1985) pp. 843–66.
15. C. YOU, A. THOMPSON and I. BERSTEIN, *Scripta Metall.* **21** (1987) 181.

Received 3 August
and accepted 12 October 1992